Available online at www.sciencedirect.com
ScienceDirect
Journal of Solid State Chemistry 181 (2008) 217–220
JOURNAL OF SOLID STATE CHEMISTRY
www.elsevier.com/locate/jssc

Preparation and magnetic properties of Fe^{3+}–Nb^{5+} co-doped SnO_2

Yu Wang, Guangsheng Pang*, Yan Chen, Shihui Jiao, Dong Wang, Shouhua Feng

State Key Laboratory of Inorganic Synthesis and Preparative Chemistry, College of Chemistry, Jilin University, Changchun 130012, PR China

Received 27 August 2007; received in revised form 16 November 2007; accepted 16 November 2007
Available online 22 November 2007

Abstract

Fe^{3+}–Nb^{5+} co-doped SnO_2 was prepared at 1200 °C by a simple chemical co-precipitation method. The $Sn_{1-2x}Fe_xNb_xO_2$ solid solutions kept cassiterite structure in the range of $0<x\leqslant 0.33$, and their cell parameters decrease with increasing x. While $x=0.40$, a second phase with orthorhombic $FeNbO_4$ structure co-exists with the cassiterite phase, and the second phase becomes dominant while $x\geqslant 0.45$. The magnetic measurements indicated that low doping ratio sample ($x=0.03$) exhibits paramagnetic behavior. A paramagnetic-to-antiferromagnetic phase transition was observed for the samples with higher doping ratio ($x\geqslant 0.15$).

Keywords: SnO_2; Solid solution; Magnetic property

1. Introduction

Tin dioxide is an n-type semiconductor with a wide band gap of ~3.6 eV. Owing to its excellent electronic and optical properties, SnO_2 is widely used for applications such as resistors, gas sensors, special coating for energy-conserving "low-emissivity" windows, transparent heating elements, electrodes in glass melting furnaces, antistatic coating, etc. [1–4]. In order to improve the performance of SnO_2, dopants are introduced. For example, Nb_2O_5 is used as additive to control particle size and particle-size distribution of SnO_2 [5]. Introducing some transition metals or their oxides can improve the sensitivity and selectivity of SnO_2-based sensors, and have a strong effect on the electronic and catalytic properties of SnO_2 surface [6,7].

In recent years, considerable attention was focused on Fe-doped SnO_2 materials, since they exhibit room temperature ferromagnetism, which has potential use in spintronics applications [8]. Although a variety of methods were used to prepare Fe-doped SnO_2, such as Pechini's method [9], hydrothermal synthesis [10], chemical co-precipitation [11], etc., the solubility of Fe in SnO_2 is still low and the reported solubility limit is 10% [12,13]. Because of the corundum-type structure, α-Fe_2O_3 has no tendency to form solid solutions with rutile-type SnO_2, although Sn^{4+} and Fe^{3+} have similar ionic radius [9,12]. Moreover, substitution of Fe^{3+} for Sn^{4+} results in the formation of oxygen vacancy to compensate the charge balance in the lattice. Oxygen vacancies are unstable at high temperature, and Fe dopants diffuse towards the surface of the particles prepared at temperature above 600 °C [8]. Thus, maintaining the charge balance is favorable to improve the solubility of Fe in SnO_2. Abakumov and co-workers reported that single-phase samples of $Sn_{2-2x}Sb_xFe_xO_4$ ($0.26\leqslant x\leqslant 0.66$) solid solution could be prepared by solid-state reaction at 1300 °C in air [14]. In this paper, we report the preparation and magnetic properties of Fe^{3+}–Nb^{5+} co-doped SnO_2 by a simple chemical co-precipitation method.

2. Experimental section

$Sn_{1-2x}Fe_xNb_xO_2$ solid solutions were prepared by a chemical co-precipitation method. NH_4OH (25 wt%), HCl (36 wt%), $SnCl_4\cdot 5H_2O$ (99.0%), and $FeCl_3\cdot 6H_2O$ (99.0%) were of analytical grade and purchased from Beijing Chemical Reagent Corp., $NbCl_5$ (99.0%) was

*Corresponding author.
E-mail address: panggs@jlu.edu.cn (G. Pang).

0022-4596/$ - see front matter © 2007 Elsevier Inc. All rights reserved.
doi:10.1016/j.jssc.2007.11.019

purchased from Aldrich. All chemicals were used as received without any further purification. In a typical procedure for the preparation of $Sn_{0.70}Fe_{0.15}Nb_{0.15}O_2$, 8.760 g $SnCl_4 \cdot 5H_2O$ and 1.448 g $FeCl_3 \cdot 6H_2O$ were dissolved in 500 ml de-ionized water to form a clear solution. Then, 1.447 g $NbCl_5$, which was dissolved in 15 ml HCl (36 wt%), was added to the above solution. With vigorously stirring, the NH_4OH solution (5 M) was dropped slowly until the pH value reached 8. The resulting precipitate was centrifuged and washed several times with de-ionized water, and dried at 70 °C overnight. The product was ground and pressed into pellet under 4 ton/cm^2. Finally, the pellet was sintered in alumina crucibles at 1200 °C for 2 h, and cooled to room temperature naturally.

Powder X-ray diffraction (XRD) analysis was performed on a Rigaku D/MAX 2500/PC X-ray diffractometer with Cu$K\alpha$ radiation at 40 kV and 200 mA, and collected at a scan rate of 1.6 °/min. The simulation and analysis of the XRD patterns were performed by utilizing JADE software. Magnetic susceptibilities were measured using an MPMS-XL SQUID (Quantum Design, Inc.) magnetometer in field-cooled mode from 4 to 300 K.

3. Results and discussion

Fig. 1 shows XRD patterns of $Sn_{1-2x}Fe_xNb_xO_2$ with x-values ranging from 0 to 0.5. For the sample $x = 0$, the XRD pattern can be well indexed into tetragonal SnO_2 cassiterite structure (JCPDS 41-1445), and the samples keep cassiterite structure until $x = 0.33$. While $x = 0.40$, a second phase with orthorhombic $FeNbO_4$ structure (JCPDS 16-0358) co-exists with the cassiterite phase, and the second phase becomes dominant at $x \geqslant 0.45$. The cell parameters of $Sn_{1-2x}Fe_xNb_xO_2$ solid solutions with $0 < x \leqslant 0.33$ are listed in Table 1. The cell parameters

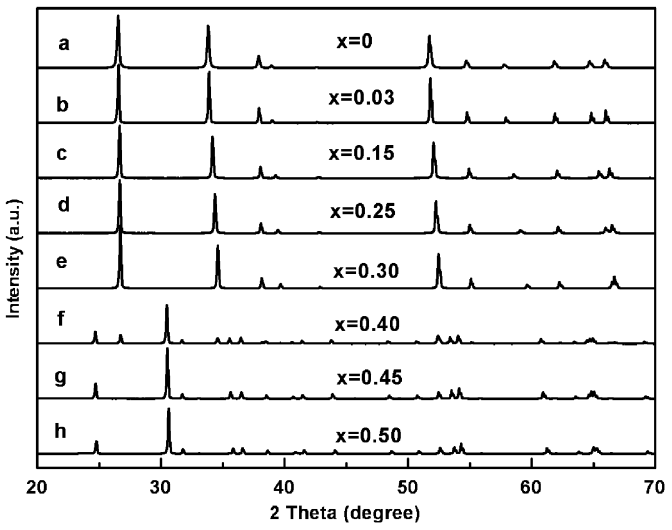

Fig. 1. X-ray diffraction patterns of $Sn_{1-2x}Fe_xNb_xO_2$ samples sintered at 1200 °C for 2 h: (a) $x = 0$, (b) $x = 0.03$, (c) $x = 0.15$, (d) $x = 0.25$, (e) $x = 0.33$, (f) $x = 0.40$, (g) $x = 0.45$, (h) $x = 0.50$.

Table 1
Unit cell parameters for the $Sn_{1-2x}Fe_xNb_xO_2$ samples

$Sn_{1-2x}Fe_xNb_xO_2$	a (Å)	c (Å)	V (Å^3)
$x = 0$	4.7368(9)	3.1861(1)	71.49
$x = 0.03$	4.7351(2)	3.1806(5)	71.31
$x = 0.06$	4.7321(1)	3.1734(5)	71.06
$x = 0.10$	4.7284(6)	3.1632(5)	70.72
$x = 0.15$	4.7241(4)	3.1501(1)	70.30
$x = 0.20$	4.7192(4)	3.1365(1)	69.85
$x = 0.25$	4.7157(0)	3.1219(8)	69.43
$x = 0.30$	4.7109(4)	3.1073(2)	68.96
$x = 0.33$	4.7093(3)	3.0971(2)	68.69

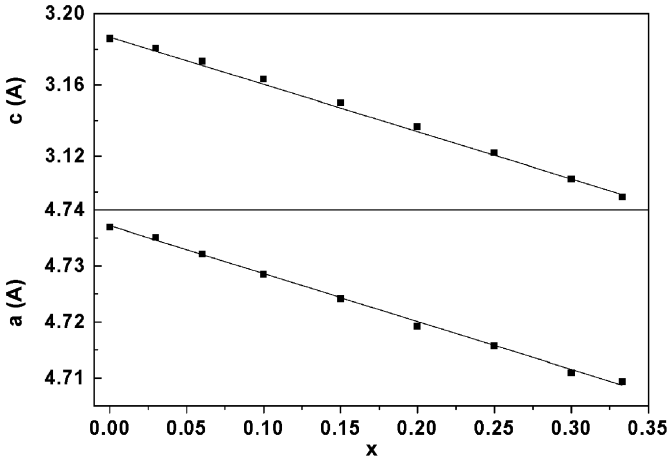

Fig. 2. Variations of the unit cell parameters vs. composition x for $Sn_{1-2x}Fe_xNb_xO_2$ samples.

decrease linearly with increasing x (Fig. 2). This result confirms the substitution of Sn^{4+} ($r = 0.83$ Å, CN = 6) by Nb^{5+} ($r = 0.78$ Å, CN = 6) and Fe^{3+} ($r = 0.79$ Å, CN = 6, high spin). The tendency of surface segregation of Fe^{3+} is inhibited because of the charge balance due to the substitution of two Sn^{4+} by one Nb^{5+} and one Fe^{3+} in the $Sn_{1-2x}Fe_xNb_xO_2$ solid solutions. The doping ratio of Fe^{3+} in SnO_2 can be significantly increased up to 0.33 by co-doping with Nb^{5+}.

There is the possibility that the SnO_2-based solid solutions demix into two rutile-type phases with close unit cell parameters and slightly different compositions [15]. The demixing into two similar rutile-type phases would result in a broadening of the X-ray powder diffraction peaks due to a small difference in cell parameters of the constituting phases. There should be an abnormality in the plot of the full-width at half-maximum (FWHM) of the reflections vs. 2θ angle for the demixed sample. As shown in Fig. 3, the samples with $x = 0.06$, 0.15, and 0.33 exhibit similar dependencies of FWHM on 2θ. This confirmed that there are no phases demixing in the $Sn_{1-2x}Fe_xNb_xO_2$ solid solutions with $0 < x \leqslant 0.33$ prepared at 1200 °C.

Fig. 4(a) shows the temperature dependence of magnetizations for the $Sn_{1-2x}Fe_xNb_xO_2$ solid solutions with

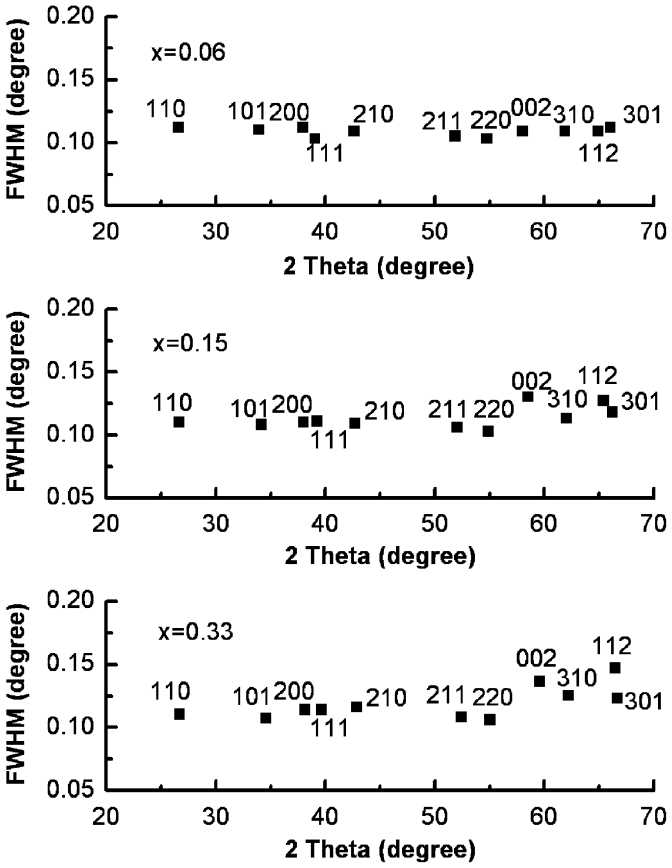

Fig. 3. The plots of FWHM vs. 2θ for the $Sn_{1-2x}Fe_xNb_xO_2$ samples ($x = 0.06$, 0.15, and 0.33). Miller indexes $h\,k\,l$ are marked.

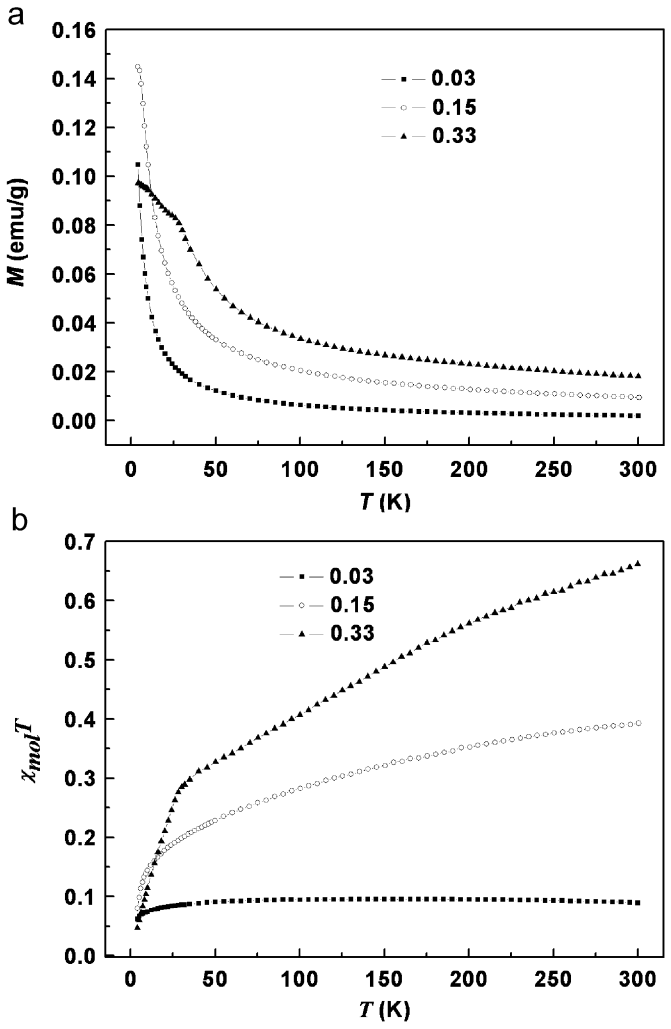

Fig. 4. (a) The plots of magnetization vs. temperature taken at 1000 Oe for $Sn_{1-2x}Fe_xNb_xO_2$ samples ($x = 0.03$, 0.15, and 0.33). (b) Plots of $\chi_m T$ vs. T.

$x = 0.03$, 0.15, and 0.33. Fig. 4(b) shows the χT–T curves of these three samples. According to the Curie–Weiss law:

$$\chi = \frac{C(x)}{T - \theta(x)},$$

where $C(x) = xN(g\mu_B)^2 S(S+1)/3u_B$ for considering only nearest neighbor interactions. The sample with $x = 0.03$ shows paramagnetic behavior at low temperature (4–225 K), and $C(x = 0.03) = 0.097$ is obtained from the fitting line in the $1/\chi$–T curve, as shown in Fig. 4(a). Above 225 K, the nonlinear part of the $1/\chi$–T curve is due to the diamagnetism of SnO_2, which influences the net magnetic moment of the sample.

Antiferromagnetic property was observed for the samples with $x = 0.15$ and 0.33 as shown in Fig. 5(b) and (c), respectively. With the doping ratio of Fe^{3+} and Nb^{5+} increasing, the antiferromagnetic property of the solid solutions became more obvious. The linear parts of $1/\chi$–T curves of the samples with $x = 0.15$ and 0.33 follow a Curie–Weiss-type behavior with a negative intercept on the temperature axis ($\theta = -83.2$ for $x = 0.15$, $\theta = -155.4$ for $x = 0.33$). The value of the effective Bohr magnetron number is 4.90 μ_B for $x = 0.33$ and 5.17 μ_B for $x = 0.15$ as against the expected spin only moment of Fe^{3+} (5.92 μ_B). The experimental value is below the theoretical paramagnetic value, which indicates that Fe^{3+} ion substituting for Sn^{4+} ion is antiferromagnetic coupled. The observed antiferromagnetic behaviors may originate from the antiferromagnetic coupling of Fe^{3+} ions in $Sn_{1-2x}Fe_xNb_xO_2$ samples.

4. Conclusions

In summary, the solubility of Fe^{3+} in SnO_2 has been increased up to 33% by co-doping with Nb^{5+}. The $Sn_{1-2x}Fe_xNb_xO_2$ ($0 < x \leqslant 0.33$) solid solutions could be prepared at 1200 °C by a simple chemical co-precipitation method. The cassiterite structure is stabilized because of the charge balance due to the substitution of two Sn^{4+} by one Nb^{5+} and one Fe^{3+}. The magnetic measurements indicated that low doping ratio sample ($x = 0.03$) exhibits paramagnetic behavior. A paramagnetic-to-antiferromagnetic phase transition is observed for the samples with higher doping ratio ($x \geqslant 0.15$).

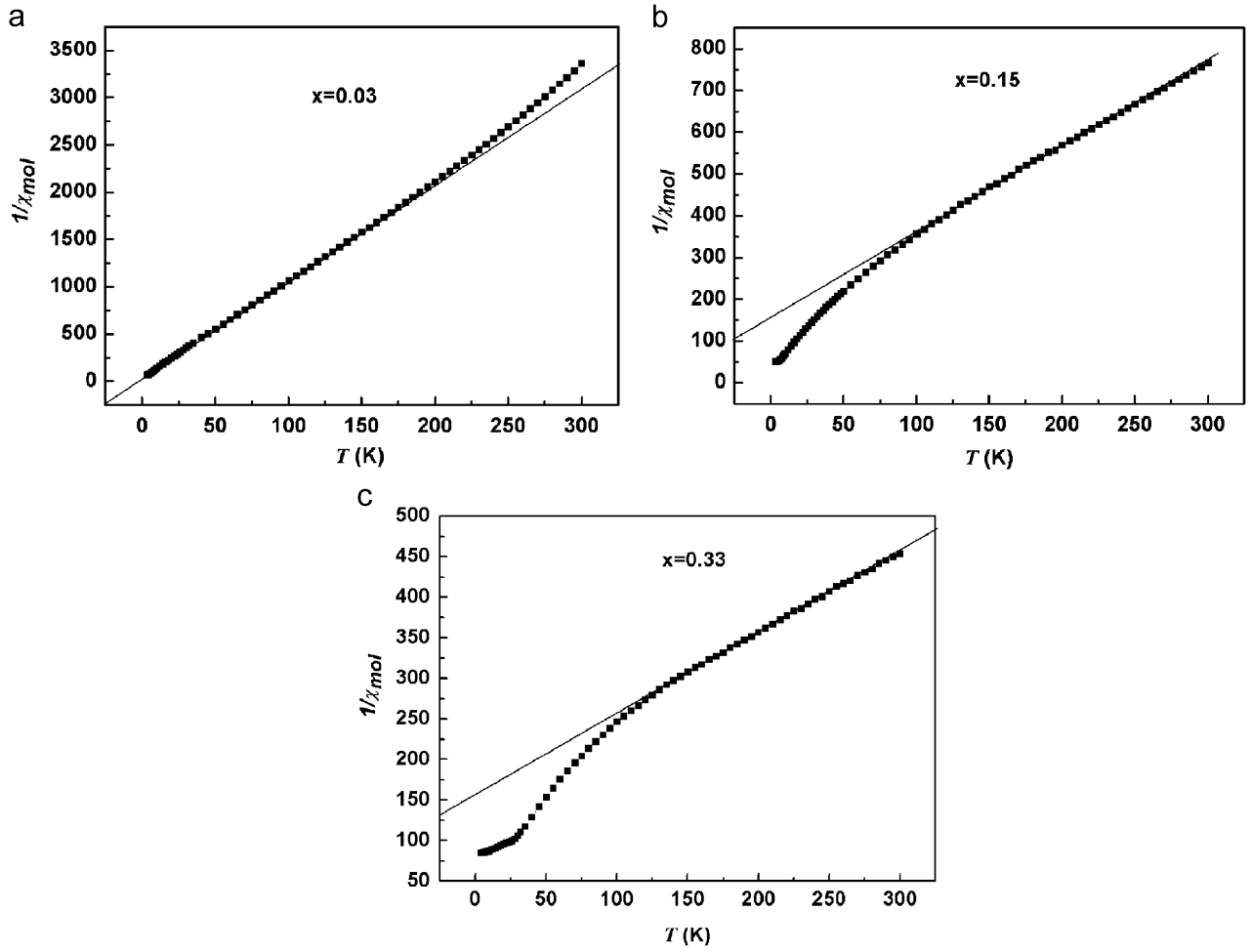

Fig. 5. The plots of inverse magnetic susceptibility vs. temperature: (a) $x = 0.03$, (b) $x = 0.15$, (c) $x = 0.33$.

Acknowledgments

This research was supported by the National Natural Science Foundation of China (nos. 20671039 and 20121103) and the National High Technology Research and Development Program of China (863 Program).

References

[1] H. Ogawa, A. Abe, M. Nishikawa, S. Hayakawa, J. Electrochem. Soc. 128 (1981) 2020.
[2] N.J. Arfsten, R. Kaufmann, H. Dislich, in: Proceedings of the International Conference on Ultrastructure Processing of Ceramics Glass and Composites, Gainesville, FL, 1983, Wiley, New York, 1984, p. 189.
[3] Z.M. Jarzebski, J.P. Marton, J. Electrochem. Soc. 123 (1976) 299c.
[4] Z.M. Jarzebski, J.P. Marton, J. Electrochem. Soc. 123 (1976) 333c.
[5] E.R. Leite, I.T. Weber, E. Longo, J.A. Varela, Adv. Mater. 12 (2000) 965.
[6] M.N. Rumyantseva, O.V. Safonova, M.N. Boulova, L.I. Ryabova, A.M. Gas′kov, Russ. Chem. Bull., Int. Ed. 52 (2003) 1217.
[7] P. Hidalgo, R.H.R. Castro, A.C.V. Coelho, D. Gouvêa, Chem. Mater. 17 (2005) 4149.
[8] A. Punnoose, J. Hays, A. Thurber, M.H. Engelhard, R.K. Kukkadapu, C. Wang, V. Shutthanandan, S. Thevuthasan, Phys. Rev. B 72 (2005) 054402.
[9] R.H.R. Castro, P. Hidalgo, J.A.H. Coaquira, J. Bettini, D. Zanchet, D. Gouvêa, Eur. J. Inorg. Chem. (2005) 2134.
[10] M. Sorescua, L. Diamandescua, D. Tarabasanu-Mihailab, V.S. Teodorescu, B.H. Howard, J. Phys. Chem. Solids 65 (2004) 1021.
[11] J.B. Wang, M.G. Yang, Y.M. Li, L.C. Chen, Y. Zhang, B.J. Ding, J. Non-Cryst. Solids 351 (2005) 228.
[12] B. Lu, C. Wang, Y. Zhang, Appl. Phys. Lett. 70 (1997) 717.
[13] S. Musić, S. Popović, M. Metikoš-Huković, V. Gvozdić, et al., J. Mater. Sci. Lett. 10 (1991) 197.
[14] V.A. Govorov, A.M. Abakumov, M.G. Rozova, A.G. Borzenko, S.Y. Vassiliev, V.M. Mazin, M.I. Afanasov, P.B. Fabritchnyi, G.A. Tsirlina, E.V. Antipov, Chem. Mater. 17 (2005) 3004.
[15] A. Martinelli, M. Ferretty, Mater. Res. Bull. 38 (2003) 1629.